

New Simulation Models for Non-Isotropic Scattering Mobile-to-Mobile Rayleigh Fading Channels

Xiang Cheng
Joint Research Institute for
Signal and Image Processing
School of EPS
Heriot-Watt University
Edinburgh, EH14 4AS, UK
xc48@hw.ac.uk

Cheng-Xiang Wang
Joint Research Institute for
Signal and Image Processing
School of EPS
Heriot-Watt University
Edinburgh, EH14 4AS, UK
cheng-
xiang.wang@hw.ac.uk

David I. Laurenson
Joint Research Institute for
Signal and Image Processing
Institute for Digital
Communications
University of Edinburgh
Edinburgh, EH9 3JL, UK
dave.laurenson@ed.ac.uk

Sana Salous
Center for Communication
Systems
University of Durham
Durham, DH1 3LE, UK
sana.salous@durham.ac.uk

Athanasios V. Vasilakos
Department of Computer and
Telecommunications
Engineering
University of Western
Macedonia
Kozani, GR 50100, Greece
vasilako@ath.forthnet.gr

ABSTRACT

To simulate mobile-to-mobile (M2M) Rayleigh fading channels under more realistic scenario of non-isotropic scattering, we propose one deterministic and one stochastic sum-of-sinusoids (SoS) based simulation models. The proposed models extensively consider the distributions of the angle of arrival (AoA) and the angle of departure (AoD), and thus show a good approximation to the desired statistical properties of the reference model.

Categories and Subject Descriptors

G.3 [Probability and Statistics]: Stochastic processes;
H.1 [Models and Principles]: Miscellaneous

General Terms

Algorithms, Design, Theory

Keywords

Channel simulation model, mobile-to-mobile communications, Rayleigh fading, sum-of-sinusoids, non-isotropic scattering

1. INTRODUCTION

In recent years, M2M communications have received increasing attention due to some new applications, such as

Permission to make digital or hard copies of all or part of this work for personal or classroom use is granted without fee provided that copies are not made or distributed for profit or commercial advantage and that copies bear this notice and the full citation on the first page. To copy otherwise, to republish, to post on servers or to redistribute to lists, requires prior specific permission and/or a fee.

VehiCom'09, co-located with IWCMC'09, June 21–24, 2009, Leipzig, Germany.

Copyright 2009 ACM 978-1-60558-569-7/09/06 ...\$5.00.

wireless mobile ad hoc networks, relay-based cellular networks, and dedicated short range communications (DSRC) for intelligent transportation systems (IEEE 802.11p). Such M2M systems consider that both the transmitter (Tx) and receiver (Rx) are in motion and equipped with low elevation antennas. To successfully analyze and design such M2M systems, it is necessary to have proper reference models for the underlying propagation channels. Many M2M reference channel models were proposed for both isotropic scattering environments, e.g., those in [1] and [2], and more realistic non-isotropic scattering environments, e.g., those in [3]–[5].

Besides the modeling of a M2M channel and the investigation of its statistical properties, the development of accurate M2M channel simulation models also plays a major role in the practical simulation and performance evaluation of M2M systems. However, up to now, many M2M Rayleigh channel simulators [6]–[8] are limited to isotropic scattering environments, while simulation models for M2M channels under a more realistic scenario of non-isotropic scattering are scarce in the current literature. To the best of the authors' knowledge, only one stochastic SoS based simulation model [9] was proposed for the simulation of non-isotropic scattering M2M Rayleigh fading channels. However, the model did not completely utilize the distributions of the AoA and AoD (i.e., only considered the symmetrical property of the distributions) and was designed based on the acceptance rejection algorithm (AJA). This leads to the AJA model having a notable difficulty in reproducing the desired statistical properties of the reference model and a comparatively high numerical computation expenditure. Furthermore, it is worth noting that accurate deterministic simulation models for non-isotropic scattering M2M Rayleigh fading channels are not available in the current literature.

To fill the above gap, in this paper based on the “double-ring” concept, originated from [7] for isotropic scattering M2M Rayleigh fading channels, we first propose a new M2M

deterministic SoS based simulation model, where all the three key parameters (e.g., gains, frequencies, and phases) are fixed for all simulation trials. By allowing at least one parameter (frequencies and/or gains) to be a random variable, our deterministic model can be further modified to a stochastic model. It is worth noting that the proposed simulation models extensively consider the probability density functions (PDFs) of the AoA and AoD, and thus can approximate the desired statistical properties of the reference model for any non-isotropic scattering M2M Rayleigh fading channel. Moreover, compared to the AJA stochastic model in [9], our stochastic model presents better approximation to the desired properties of the reference model with an even smaller number of harmonic functions.

The paper is structured as follows. Section 2 gives a brief description of the reference model for non-isotropic scattering M2M Rayleigh fading channels. In Section 3, we propose two new SoS based simulation models (deterministic and stochastic models). The validation of our models are presented in Section 4. Finally, conclusions are drawn in Section 5.

2. REFERENCE MODEL

Using Akki and Haber's mathematical model [1] and considering the impact of the moving directions of the Tx and Rx, we can express the complex faded envelope of our reference model, under a narrowband non-isotropic scattering M2M Rayleigh fading assumption, as

$$h(t) = \lim_{N \rightarrow \infty} \frac{1}{\sqrt{N}} \sum_{n=1}^N e^{j\psi_n} \times e^{j[2\pi f_{Tmax} t \cos(\phi_T^n - \gamma_T) + 2\pi f_{Rmax} t \cos(\phi_R^n - \gamma_R)]} \quad (1)$$

where $j = \sqrt{-1}$, N is the number of propagation paths, f_{Tmax} and f_{Rmax} are the maximum Doppler frequency due to the motion of the Tx and Rx, respectively. The Tx and Rx move in directions determined by the angles of motion γ_T and γ_R , respectively. The random AoA and AoD of the n th path are denoted by ϕ_R^n and ϕ_T^n , respectively, and ψ_n is the random phase uniformly distributed on $[-\pi, \pi]$. It is assumed that ϕ_R^n , ϕ_T^n , and ψ_n are mutually independent random variables.

Since the number of effective scatterers in the reference model $h(t)$ tends to infinity, the discrete AoA ϕ_R^n and AoD ϕ_T^n , can be replaced by continuous random variables ϕ_R and ϕ_T , respectively. Note that since $h(t)$ describes a non-isotropic scattering M2M Rayleigh fading channel the AoA ϕ_R and AoD ϕ_R exhibit nonuniform distributions. In the literature, many different nonuniform distributions have been proposed to characterize the AoA ϕ_R and AoD ϕ_R , such as the Gaussian, wrapped Gaussian, and cardioid PDFs [11]. In this paper, the von Mises PDF [12] is used, which can approximate all the aforementioned PDFs. The von Mises PDF is defined as $f(\phi) \triangleq \exp[k \cos(\phi - \mu)] / [2\pi I_0(k)]$, where $\phi \in [-\pi, \pi]$, $I_0(\cdot)$ is the zeroth-order modified Bessel function of the first kind, $\mu \in [-\pi, \pi]$ accounts for the mean value of the angle ϕ , and k ($k \geq 0$) is a real-valued parameter that controls the angle spread of the angle ϕ . For $k=0$ (isotropic scattering), the von Mises PDF reduces to the uniform distribution, while for $k > 0$ (non-isotropic scattering), the von Mises PDF approximates different distributions based on the values of k [12].

Applying the von Mises PDF for the reference model $h(t)$ in (1), we obtain $f(\phi_R) \triangleq \exp[k_R \cos(\phi_R - \mu_R)] / [2\pi I_0(k_R)]$ for the AoA ϕ_R and $f(\phi_T) \triangleq \exp[k_T \cos(\phi_T - \mu_T)] / [2\pi I_0(k_T)]$ for the AoD ϕ_T . Considering these two von Mises PDFs, we can express the correlation function (CF) of the reference model as [4]

$$\rho_{hh}(\tau) = \mathbf{E}[h(t) h^*(t - \tau)] = \frac{1}{I_0(k_T) I_0(k_R)} I_0 \left[(A_T^2 + B_T^2)^{1/2} \right] I_0 \left[(A_R^2 + B_R^2)^{1/2} \right] \quad (2)$$

$$\text{with } A_T = -k_T \cos(\mu_T) - j2\pi\tau f_{Tmax} \cos(\gamma_T) \quad (3a)$$

$$B_T = -k_T \sin(\mu_T) - j2\pi\tau f_{Tmax} \sin(\gamma_T) \quad (3b)$$

$$A_R = -k_R \cos(\mu_R) - j2\pi\tau f_{Rmax} \cos(\gamma_R) \quad (3c)$$

$$B_R = -k_R \sin(\mu_R) - j2\pi\tau f_{Rmax} \sin(\gamma_R) \quad (3d)$$

where $(\cdot)^*$ denotes the complex conjugate operation and $\mathbf{E}[\cdot]$ is the stochastic expectation operator.

3. NEW SIMULATION MODELS

In this section, based on the reference model introduced in Section 2, we will propose the corresponding SoS based deterministic and stochastic simulation models. The essential issue to design a M2M SoS based simulation model is to find the sets of AoAs $\{\bar{\phi}_R^{(n)}\}_{n=1}^N$ and AoDs $\{\bar{\phi}_T^{(n)}\}_{n=1}^N$ that make the simulation model reproduce the desired statistical properties of the reference model as faithfully as possible with reasonable complexity, i.e., with a finite number of N . Here, $\bar{\phi}_R^{(n)}$ and $\bar{\phi}_T^{(n)}$ denote the AoA and AoD of a simulation model, respectively. Under the condition of non-isotropic scattering environments, the PDFs of the AoA ϕ_R and AoD ϕ_T should be extensively considered for the proper design of the sets of AoAs $\{\bar{\phi}_R^{(n)}\}_{n=1}^N$ and AoDs $\{\bar{\phi}_T^{(n)}\}_{n=1}^N$ that guarantee the uniqueness of the sine and cosine functions related to the AoA $\bar{\phi}_R^{(n)}$ and AoD $\bar{\phi}_T^{(n)}$ in a complex faded envelope. This means that the design of the sets of AoAs and AoDs for the complex faded envelope $h(t)$ in (1) should meet the following two conditions: 1) $\cos(\bar{\phi}_R^{(n)} - \gamma_R) \neq \cos(\bar{\phi}_R^{(m)} - \gamma_R)$, $n \neq m$; and 2) $\cos(\bar{\phi}_T^{(n)} - \gamma_T) \neq \cos(\bar{\phi}_T^{(m)} - \gamma_T)$, $n \neq m$.

3.1 New Deterministic Simulation Model

Following the above mentioned two conditions with the consideration of the PDFs of the AoA and AoD, and applying the "double-ring" concept in [7], we design a new deterministic simulation model as follows

$$\tilde{h}(t) = \tilde{h}_i(t) + j\tilde{h}_q(t) \quad (4)$$

$$\tilde{h}_i(t) = \frac{1}{\sqrt{N_i M_i}} \sum_{n_i, m_i=1}^{N_i, M_i} \cos \left[\tilde{\psi}_{n_i m_i} + 2\pi f_{Tmax} t \cos(\tilde{\phi}_T^{m_i} - \gamma_T) + 2\pi f_{Rmax} t \cos(\tilde{\phi}_R^{n_i} - \gamma_R) \right] \quad (5)$$

$$\tilde{h}_q(t) = \frac{1}{\sqrt{N_q M_q}} \sum_{n_q, m_q=1}^{N_q, M_q} \sin \left[\tilde{\psi}_{n_q m_q} + 2\pi f_{Tmax} t \cos(\tilde{\phi}_T^{m_q} - \gamma_T) + 2\pi f_{Rmax} t \cos(\tilde{\phi}_R^{n_q} - \gamma_R) \right] \quad (6)$$

where the AoA and AoD are

$$\tilde{\phi}_R^{n_i/q} = F^{-1} \left(\frac{n_i/q - p}{N_i/q} \right), \quad \tilde{\phi}_R^{n_i/q} \in [-\pi, \pi] \quad (7a)$$

$$\tilde{\phi}_T^{m_{i/q}} = F^{-1} \left(\frac{m_{i/q} - p}{M_{i/q}} \right), \quad \tilde{\phi}_T^{m_{i/q}} \in [-\pi, \pi) \quad (7b)$$

with $F^{-1}(\cdot)$ denoting the inverse function of the von Mises cumulative distribution function (CDF). In (4)–(6), $\tilde{h}_i(t)$ and $\tilde{h}_q(t)$ are inphase and quadrature components of complex envelope $\tilde{h}(t)$, respectively, $N_{i/q}$ is the number of effective scatterers located on the ring around the RX, $M_{i/q}$ is the number of effective scatterers located on the ring around the Tx, the phases $\tilde{\psi}_{n_{i/q}m_{i/q}}$ are random variables uniformly distributed on the interval $[-\pi, \pi)$. It is assumed that $\tilde{\phi}_R^{n_{i/q}}$, $\tilde{\phi}_T^{m_{i/q}}$, and $\tilde{\psi}_{n_{i/q}m_{i/q}}$ are mutually independent. Note that $\tilde{h}(t)$ is ergodic random process and the sets of AoAs and AoDs are constant for different simulations. Based on the PDFs of the AoA and AoD (i.e., the mean AoA μ_R and mean AoD μ_T), and the angles of motion γ_R and γ_T , the values of the parameters $N_{i/q}$, $M_{i/q}$, and p can be determined as the following.

- *Case I*: The values of μ_T , μ_R , γ_T , and γ_R meet the following condition: $|\mu_T - \gamma_T| = |\mu_R - \gamma_R| = 90^\circ$. In such a case, we have $N_i \neq N_q$, $M_i \neq M_q$, and $p=1/2$, which leads to $\tilde{\phi}_R^{(n_{i/q})} = F^{-1} \left(\frac{n_{i/q} - 1/2}{N_{i/q}} \right)$ with $[-\pi, \pi)$ and $\tilde{\phi}_T^{(m_{i/q})} = F^{-1} \left(\frac{m_{i/q} - 1/2}{M_{i/q}} \right)$ with $[-\pi, \pi)$.
- *Case II*: The values of μ_T , μ_R , γ_T , and γ_R meet the following condition: $|\mu_T - \gamma_T| = |\mu_R - \gamma_R| = 0^\circ$ or $\pm\pi$. In such a case, we have $N_i = N_q = N$, $M_i = M_q = M$, and $p=1/4$, which results in $\tilde{\phi}_R^{(n)} = F^{-1} \left(\frac{n-1/4}{N} \right)$ ($n_i = n_q = n$) with $[-\pi, \pi)$ and $\tilde{\phi}_T^{(m)} = F^{-1} \left(\frac{m-1/4}{M} \right)$ ($m_i = m_q = m$) with $[-\pi, \pi)$.
- *Case III*: The values of μ_T , μ_R , γ_T , and γ_R do not meet all the conditions in other cases. In this case, we have $N_i = N_q = N$, $M_i = M_q = M$, and $p=1/2$, which leads to $\tilde{\phi}_R^{(n)} = F^{-1} \left(\frac{n-1/2}{N} \right)$ ($n_i = n_q = n$) with $[-\pi, \pi)$ and $\tilde{\phi}_T^{(m)} = F^{-1} \left(\frac{m-1/2}{M} \right)$ ($m_i = m_q = m$) with $[-\pi, \pi)$.

A few remarks are made below in order to fully describe this model.

Remark 1: As mentioned above, the following two conditions should be met for the proper design of a M2M SoS based simulation model: 1) $\tilde{\phi}_R^{n_{i/q}} \neq -\tilde{\phi}_R^{(n'_{i/q})} + 2\gamma_R$, $n_{i/q} \neq n'_{i/q}$ and 2) $\tilde{\phi}_T^{m_{i/q}} \neq -\tilde{\phi}_T^{(m'_{i/q})} + 2\gamma_T$, $m_{i/q} \neq m'_{i/q}$. However, except for *Case II*, for other cases, it is difficult to find the sets of AoAs $\tilde{\phi}_R^{n_{i/q}}$ and AoDs $\tilde{\phi}_T^{m_{i/q}}$ to exactly meet the above two conditions. Inspired by the isotropic simulation model in [7] and based on numerous simulations, we found that $p=1/2$ results in better performance of the simulation model than that with other values of p . The validation of this model will be given in Section IV.

Remark 2: During our investigation, we found that for *Case I* the cross-correlation between the inphase component $\tilde{h}_i(t)$ and quadrature component $\tilde{h}_q(t)$ is equal to zero. By setting $N_i \neq N_q$ and $M_i \neq M_q$ in this case, we can directly use the expression of our model itself to guarantee the aforementioned cross-correlation is equal to zero rather than through the design of the AoAs and AoDs. This makes

a more efficient use of the number of harmonic functions and thus renders the model show better performance.

Remark 3: The time-average CF of the proposed simulation model $\tilde{h}(t)$ can be expressed as

$$\tilde{\rho}_{\tilde{h}\tilde{h}}(\tau) = 2\tilde{\rho}_{\tilde{h}_i\tilde{h}_i}(\tau) - 2j\tilde{\rho}_{\tilde{h}_i\tilde{h}_q}(\tau) \quad (8)$$

$$\tilde{\rho}_{\tilde{h}_i\tilde{h}_i}(\tau) = \frac{1}{2N_iM_i} \sum_{n_i, m_i=1}^{N_i, M_i} \cos \left[2\pi f_{T_{max}} \tau \cos(\tilde{\phi}_T^{m_i} - \gamma_T) + 2\pi f_{R_{max}} \tau \cos(\tilde{\phi}_R^{n_i} - \gamma_R) \right] \quad (9)$$

$$\tilde{\rho}_{\tilde{h}_i\tilde{h}_q}(\tau) = \begin{cases} 0, & N_i \neq N_q \text{ and } M_i \neq M_q \text{ (Case I)} \\ -\frac{1}{2NM} \sum_{n, m=1}^{N, M} \sin \left[2\pi f_{T_{max}} \tau \cos(\tilde{\phi}_T^m - \gamma_T) + 2\pi f_{R_{max}} \tau \cos(\tilde{\phi}_R^n - \gamma_R) \right], & N_i = N_q = N \\ & \text{and } M_i = M_q = M \text{ (Case II and III)} \end{cases} \quad (10)$$

When N (N_i) and M (M_i) tend to infinite, it is straightforward that the time-average CF in (8) matches the ensemble average CF in (2). This allows us to conclude that for $\{N(N_i), M(M_i)\} \rightarrow \infty$, our simulation model can represent correlation properties of the reference model.

3.2 New stochastic Simulation Model

By allowing both phases and frequencies to be random variables, our deterministic model can be further modified to a stochastic simulation model as

$$\hat{h}(t) = \hat{h}_i(t) + j\hat{h}_q(t) \quad (11)$$

$$\hat{h}_i(t) = \frac{1}{\sqrt{N_iM_i}} \sum_{n_i, m_i=1}^{N_i, M_i} \cos \left[\hat{\psi}_{n_i m_i} + 2\pi f_{T_{max}} t \cos(\hat{\phi}_T^{m_i} - \gamma_T) + 2\pi f_{R_{max}} t \cos(\hat{\phi}_R^{n_i} - \gamma_R) \right] \quad (12)$$

$$\hat{h}_q(t) = \frac{1}{\sqrt{N_qM_q}} \sum_{n_q, m_q=1}^{N_q, M_q} \sin \left[\hat{\psi}_{n_q m_q} + 2\pi f_{T_{max}} t \cos(\hat{\phi}_T^{m_q} - \gamma_T) + 2\pi f_{R_{max}} t \cos(\hat{\phi}_R^{n_q} - \gamma_R) \right] \quad (13)$$

where the AoA and AoD are

$$\hat{\phi}_R^{n_{i/q}} = F^{-1} \left(\frac{n_{i/q} - 1/2 + \theta_R}{uN_{i/q}} \right), \quad \hat{\phi}_R^{n_{i/q}} \in [\phi_R^l, \phi_R^r] \quad (14a)$$

$$\hat{\phi}_T^{m_{i/q}} = F^{-1} \left(\frac{m_{i/q} - 1/2 + \theta_T}{vM_{i/q}} \right), \quad \hat{\phi}_T^{m_{i/q}} \in [\phi_T^l, \phi_T^r]. \quad (14b)$$

In (11)–(13), $\hat{h}_i(t)$ and $\hat{h}_q(t)$ are inphase and quadrature components of complex envelope $\hat{h}(t)$, respectively, the phases $\hat{\psi}_{n_{i/q}m_{i/q}}$ are random variables uniformly distributed on the interval $[-\pi, \pi)$, and parameter θ_R and θ_T are random variables uniformly distributed on the interval $[-1/2, 1/2)$. Note that parameters $\hat{\phi}_R^{n_{i/q}}$, $\hat{\phi}_T^{m_{i/q}}$, $\hat{\psi}_{n_{i/q}m_{i/q}}$, θ_R and θ_T are independent of each other and $\hat{h}_{pq}(t)$ are non-ergodic random processes due to the introduction of the random variables θ_R and θ_T in the AoA $\hat{\phi}_R^{n_{i/q}}$ and AoD $\hat{\phi}_T^{m_{i/q}}$, respectively. Therefore, the sets of AoAs and AoDs vary for different simulations. The motivation behind this stochastic model originates in the model in [10] for isotropic scattering Rayleigh fading channels. Similar to our deterministic model, the values of the parameters $N_{i/q}$, $M_{i/q}$, u , v , ϕ_R^l , ϕ_R^r , ϕ_T^l , and ϕ_T^r will be determined as the following.

- *Case I*: The values of μ_T , μ_R , γ_T , and γ_R meet the following condition: $|\mu_T - \gamma_T| = |\mu_R - \gamma_R| = 90^\circ$. In such a case, we have $N_i \neq N_q$, $M_i \neq M_q$, $u = v = 1$, $\phi_R^l = 0$, $\phi_R^r = -\pi$, and $\phi_T^r = \phi_T^l = \pi$, which results in $\hat{\phi}_R^{n_i/q} = F^{-1} \left(\frac{n_i/q - 1/2 + \theta_R}{N_i/q} \right)$ with $[0, \pi)$ and $\hat{\phi}_T^{m_i/q} = F^{-1} \left(\frac{m_i/q - 1/2 + \theta_T}{M_i/q} \right)$ with $[-\pi, \pi)$.
- *Case II*: The values of μ_T , μ_R , γ_T , and γ_R meet the following condition: $\mu_T = \gamma_T = \mu_R = \gamma_R = 0^\circ$. In such a case, we have $N_i = N_q = N$, $M_i = M_q = M$, $u = v = 2$, $\phi_R^l = \phi_T^l = 0$, and $\phi_R^r = \phi_T^r = \pi$, which leads to $\hat{\phi}_R^n = F^{-1} \left(\frac{n - 1/2 + \theta_R}{2N} \right)$ ($n_i = n_q = n$) with $[0, \pi)$ and $\hat{\phi}_T^m = F^{-1} \left(\frac{m - 1/2 + \theta_T}{2M} \right)$ ($m_i = m_q = m$) with $[0, \pi)$.
- *Case III*: The values of μ_T , μ_R , γ_T , and γ_R do not meet all the conditions in other cases. In this case, we have $N_i = N_q = N$, $M_i = M_q = M$, $u = v = 1$, $\phi_R^l = \phi_T^l = -\pi$, and $\phi_R^r = \phi_T^r = \pi$, which leads to $\hat{\phi}_R^n = F^{-1} \left(\frac{n - 1/2 + \theta_R}{N} \right)$ ($n_i = n_q = n$) with $[-\pi, \pi)$ and $\hat{\phi}_T^m = F^{-1} \left(\frac{m - 1/2 + \theta_T}{M} \right)$ ($m_i = m_q = m$) with $[-\pi, \pi)$.

Three remarks are given in the following for the better description of the proposed stochastic model.

Remark 4: It is clear that different cases have different ranges of the AoA and AoD, on which the sets of AoAs $\hat{\phi}_R^{n_i/q}$ and AoDs $\hat{\phi}_T^{m_i/q}$ are designed. These ranges are chosen to guarantee a sufficient and efficient design of the sets of AoAs and AoDs for any non-isotropic M2M Rayleigh fading channels. The validation of this model will be given in Section IV. In addition, due to the similar reason given in *Remark 2*, our stochastic model is designed for *Case I* by setting $N_i \neq N_q$ and $M_i \neq M_q$ as well.

Remark 5: It can be shown that our stochastic model exhibits correlation properties of the reference model irrespective of the values of N_i/q and M_i/q , i.e., for any N_i/q and M_i/q . Appendix outlines the derivation of the CF $\hat{\rho}_{hh}(\tau)$ for the model $\hat{h}(t)$.

Remark 6: Note that the proposed stochastic model shows better performance and lower complexity than the AJA model [9]. Since in [9] the authors did not give the detailed explanation on how to generate the AoAs and AoDs for their model by using the AJA, it is impossible to reproduce this model. Therefore, to validate the above statement, in Figure 1 we compare the autocorrelation function of the real part of the AJA model obtained from Figure 5 in [9] with the one of our model. For a fair comparison, the same parameters as those used in Figure 5 in [9] are used as $f_{T_{max}} = 100$ Hz, $f_{R_{max}} = 50$ Hz, $\mu_T = \pi/4$, $\mu_R = -\pi/4$, $k_T = k_R = 3$, $\gamma_T = \gamma_R = 0^\circ$, and the number of simulation trials $N_{stat} = 10$. Note that the number of harmonic functions used in the AJA model is $N = 144$, while in our model is $N_i = M_i = 10$. From Figure 1, it is obvious that our model outperforms the AJA model with even smaller number of harmonic functions, i.e., $N_i \times M_i = 100 < N$.

4. NUMERICAL RESULTS AND ANALYSIS

In this section, we first validate the newly proposed deterministic model by using the squared error between correlation properties of the simulation model and those of the reference model. Then the validation of the proposed

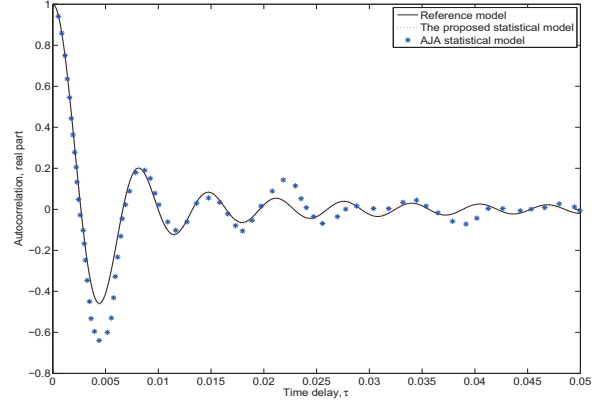


Figure 1: Comparison between the proposed stochastic model and the AJA stochastic model [9].

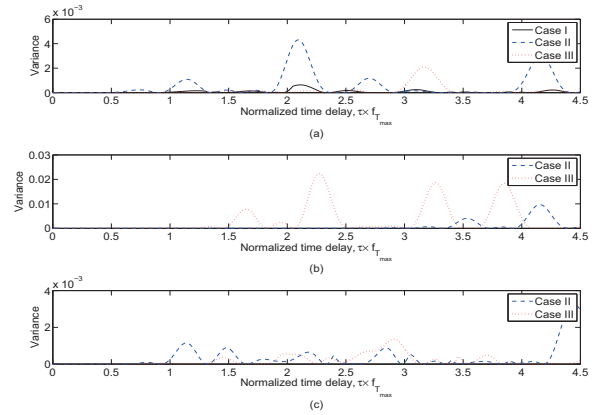


Figure 2: Variance in the CF of the proposed deterministic simulation model with $k = 1$ for different non-isotropic scattering M2M Rayleigh fading channels: (a) $\mu_T = \mu_R = 110^\circ$ and $\gamma_T = \gamma_R = 20^\circ$; (b) $\mu_T = \mu_R = \gamma_T = \gamma_R = 0^\circ$; (c) $\mu_T = 30^\circ$, $\mu_R = 160^\circ$, $\gamma_T = 10^\circ$, and $\gamma_R = 20^\circ$.

stochastic simulation model is performed by utilizing the variation in the time average properties of a single simulation trial for the stochastic model from the desired ensemble average properties. Furthermore, the performance evaluation of the proposed models is carried out by comparing the correlation properties of the proposed simulation models with those of the reference model. Unless otherwise specified, all the results presented here are obtained using $f_{T_{max}} = f_{R_{max}} = 100$ Hz, $N_i = M_i = N_q = M_q = 20$ ($N_q = M_q = 21$ for *Case I*) for the deterministic model, $N_i = M_i = N_q = M_q = 10$ ($N_q = M_q = 11$ for *Case I*) for the stochastic model, and the normalized sampling period $f_{T_{max}} T_s = 0.005$ (T_s is the sampling period).

To validate our deterministic model, in Figure 2 we compare the variance in the CF $\tilde{\rho}_{hh}(\tau)$ from the desired $\rho_{hh}(\tau)$ using the squared error $|\tilde{\rho}_{hh}(\tau) - \rho_{hh}(\tau)|^2$ for different non-isotropic M2M scenarios. Similarly, to validate our stochastic model, Figure 3 compares the variance in the time averaged CF of a single simulation trial $\check{\rho}_{hh}(\tau)$ from the desired CF $\rho_{hh}(\tau)$ as $\text{Var}[\check{\rho}_{hh}(\tau)] = \mathbf{E}[|\check{\rho}_{hh}(\tau) - \rho_{hh}(\tau)|^2]$ for dif-

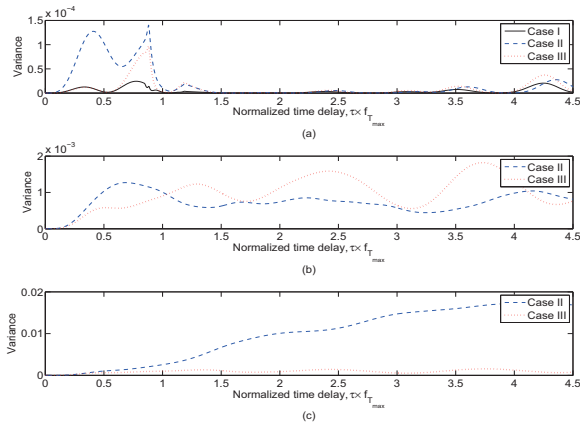


Figure 3: Variance in the CF of the proposed statistical simulation model with $k = 5$ for different non-isotropic scattering M2M Rayleigh fading channels: (a) $\mu_T = \mu_R = 110^\circ$ and $\gamma_T = \gamma_R = 20^\circ$; (b) $\mu_T = \mu_R = \gamma_T = \gamma_R = 0^\circ$; (c) $\mu_T = 20^\circ$, $\mu_R = 10^\circ$, $\gamma_T = 10^\circ$, and $\gamma_R = 20^\circ$.

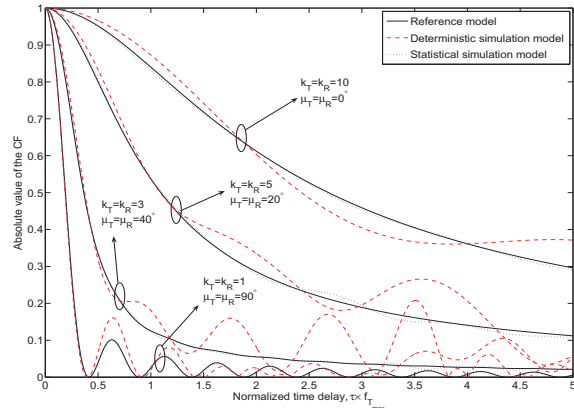


Figure 4: Comparison between the CF of the reference model and the CF of the proposed simulation models with $\gamma_T = \gamma_R = 0^\circ$ for various values of k_T , k_R , the mean AoD μ_T , and mean AoA μ_R .

ferent non-isotropic M2M scenarios. The results in Figure 3 are obtained by averaging over 10^4 simulation trials for each value of time delay τ . Note that for the sake of the readability of figures, the variance of our models for *Case I* is only shown in Figs. 2 (a) and 3 (a) since this variance is extremely large for other cases. From Figs. 2 and 3, it is clear that due to the impact of non-isotropic scattering, none set of model parameters in our models consistently outperforms others for all non-isotropic M2M scenarios. This, hence, validates the utility of our models that include three different sets of model parameters rather than only one.

To evaluate the performance of our simulation models, in Figure 4 we give a comparison between the CF of the reference model and the one of our simulation models for various values of k_T , k_R , μ_T , and μ_R . The results obtained for the stochastic model are averaged over $N_{stat} = 10$ trials. It is obvious that the deterministic model provides a fairly good approximation to the CF of the reference model, while

the stochastic model presents much better approximation with an even smaller number of complex harmonic functions $N_{i/q}$ and $M_{i/q}$.

5. CONCLUSIONS

In this paper, based on the comprehensive analysis of the PDFs of the AoA and AoD, new deterministic and stochastic SoS based simulation models have been proposed for non-isotropic M2M Rayleigh fading channels. The performance of the proposed simulation models has been verified in terms of the CF through the theoretical and simulation results. Results have shown that compared to the proposed deterministic model, the proposed stochastic model provides better approximation to the reference model with an even smaller number of harmonic functions. Moreover, our analysis has revealed that the proposed stochastic model performs better than the AJA stochastic model.

6. ACKNOWLEDGMENTS

X. Cheng, C.-X. Wang, and D. I. Laurenson acknowledge the support from the Scottish Funding Council for the Joint Research Institute in Signal and Image Processing between the University of Edinburgh and Heriot-Watt University which is a part of the Edinburgh Research Partnership in Engineering and Mathematics (ERPem).

7. REFERENCES

- [1] A. S. Akki and F. Haber, "A stochastic model for mobile-to-mobile land communication channel," *IEEE Trans. Veh. Technol.*, 35(1):2–10, Feb. 1986.
- [2] A. S. Akki, "stochastic properties of mobile-to-mobile land communication channels," *IEEE Trans. Veh. Technol.*, 43(4):826–831, Nov. 1994.
- [3] A. G. Zajić and G. L. Stüber, "Space-time correlated mobile-to-mobile channels: modelling and simulation," *IEEE Trans. Veh. Technol.*, 57(2):715–726, Mar. 2008.
- [4] X. Cheng, C.-X. Wang, D. I. Laurenson, H. H. Chen, and A. V. Vasilakos, "A generic geometrical-based MIMO mobile-to-mobile channel model," *IEEE IWCMC'08*, pages 1000–1005. Chania Crete Island, Greece, Aug. 2008.
- [5] X. Cheng, C.-X. Wang, D. I. Laurenson, and A. V. Vasilakos, "Second order statistics of non-isotropic mobile-to-mobile Ricean fading channels," *Proc. IEEE ICC'09*, Dresden, Germany, Jun. 2009, accepted for publication.
- [6] R. Wang and D. Cox, "Channel modeling for ad hoc mobile wireless networks," *IEEE VTC'02-Spring*, pages 21–25. Birmingham, USA, May 2002.
- [7] C. S. Patel, G. L. Stüber, and T. G. Pratt, "Simulation of Rayleigh-faded mobile-to-mobile communication channels," *IEEE Trans. Commun.*, 53(11):1876–1884, Nov. 2005.
- [8] A. G. Zajić and G. L. Stüber, "A new simulation model for mobile-to-mobile Rayleigh fading channels," *IEEE WCNC'06*, pages 1266–1270. Las Vegas, USA, Apr. 2006.
- [9] Y. R. Zheng, "A non-isotropic model for mobile-to-mobile fading channel simulations," *IEEE MCC'06*, pages 1–6. Washington, USA, Oct. 2006.
- [10] Y. R. Zheng and C. S. Xiao, "Improved models for the generation of multiple uncorrelated Rayleigh fading

waveforms," *IEEE Commun. Lett.*, 6(6):256–258, Jun. 2002.

- [11] X. Cheng, C.-X. Wang, and D. I. Laurenson, "A generic space-time-frequency correlation model and its corresponding simulation model for MIMO wireless channels," *Proc. EuCAP'07*, pages 1–6. Edinburgh, UK, Nov. 2007.
- [12] A. Abdi, J. A. Barger, and M. Kaveh, "A parametric model for the distribution of the angle of arrival and the associated correlation function and power spectrum at the mobile station," *IEEE Trans. Veh. Technol.*, 51(3):425–434, May 2002.
- [13] I. S. Gradshteyn, and I. M. Ryzhik, *Table of Integrals, Series, and Products*. 5th ed, A. Jeffrey, Ed. San Diego, CA: Academic, 1994.

APPENDIX

DERIVATION OF THE CF $\hat{\rho}_{\hat{h}\hat{h}}(\tau)$

In this appendix, we derive the CF $\hat{\rho}_{\hat{h}\hat{h}}(\tau)$ for the stochastic simulation model in (11)

$$\hat{\rho}_{\hat{h}\hat{h}}(\tau) = E[\hat{h}(t)\hat{h}^*(t-\tau)]$$

$$\begin{aligned} & \left\{ \frac{1}{2N_i M_i} \sum_{n_i, m_i=1}^{N_i, M_i} \int \int \cos\left\{2\pi\tau \left[f_{T_{max}} \cos\left[F^{-1}\left(\frac{m_i-1/2+\theta_T}{M_i}\right) - \gamma_T\right] \right. \right. \right. \\ & \left. \left. \left. + f_{R_{max}} \cos\left[F^{-1}\left(\frac{n_i-1/2+\theta_R}{N_i}\right) - \gamma_R\right] \right] \right\} d\theta_T d\theta_R + \frac{1}{2N_q M_q} \right. \\ & \times \left. \sum_{n_q, m_q=1}^{N_q, M_q} \int \int \cos\left\{2\pi\tau \left[f_{T_{max}} \cos\left[F^{-1}\left(\frac{m_q-1/2+\theta_T}{M_q}\right) - \gamma_T\right] \right. \right. \right. \\ & \left. \left. \left. + f_{R_{max}} \cos\left[F^{-1}\left(\frac{n_q-1/2+\theta_R}{N_q}\right) - \gamma_R\right] \right] \right\} d\theta_T d\theta_R, \quad (Case I) \right. \\ & \left. \frac{1}{NM} \sum_{n, m=1}^{N, M} \int \int e^{j2\pi\tau f_{T_{max}} \cos\left[F^{-1}\left(\frac{m-1/2+\theta_T}{M}\right) - \gamma_T\right]} \right. \\ & \times \left. e^{j2\pi\tau f_{R_{max}} \cos\left[F^{-1}\left(\frac{n-1/2+\theta_R}{N}\right) - \gamma_R\right]} d\theta_T d\theta_R, \quad N_i=N_q=N \right. \\ & \left. \text{and } M_i=M_q=M \quad (Case II \text{ and III}) \right. \\ & \left. \frac{N_i M_i}{2N_i M_i} \sum_{n_i, m_i=1}^{N_i, M_i} \int_{F^{-1}\left(\frac{n_i-1}{N_i}\right)}^{F^{-1}\left(\frac{n_i}{N_i}\right)} \int_{F^{-1}\left(\frac{m_i-1}{M_i}\right)}^{F^{-1}\left(\frac{m_i}{M_i}\right)} \cos\left\{2\pi\tau \left[f_{T_{max}} \cos(\beta_T^{m_i} - \gamma_T) + \right. \right. \right. \\ & \left. \left. \left. f_{R_{max}} \cos(\beta_R^{n_i} - \gamma_R) \right] \right\} \frac{e^{k_T \cos(\beta_T^{m_i} - \mu_T) + k_R \cos(\beta_R^{n_i} - \mu_R)}}{4\pi^2 I_0(k_T) I_0(k_R)} d\beta_T^{m_i} d\beta_R^{n_i} \right. \\ & \left. + \frac{N_q M_q}{2N_q M_q} \sum_{n_q, m_q=1}^{N_q, M_q} \int_{F^{-1}\left(\frac{n_q-1}{N_q}\right)}^{F^{-1}\left(\frac{n_q}{N_q}\right)} \int_{F^{-1}\left(\frac{m_q-1}{M_q}\right)}^{F^{-1}\left(\frac{m_q}{M_q}\right)} \cos\left\{2\pi\tau \left[f_{T_{max}} \cos(\beta_T^{m_q} - \gamma_T) + \right. \right. \right. \\ & \left. \left. \left. f_{R_{max}} \cos(\beta_R^{n_q} - \gamma_R) \right] \right\} \frac{e^{k_T \cos(\beta_T^{m_q} - \mu_T) + k_R \cos(\beta_R^{n_q} - \mu_R)}}{4\pi^2 I_0(k_T) I_0(k_R)} d\beta_T^{m_q} d\beta_R^{n_q} \right. \\ & \left. \frac{NM}{NM} \sum_{n, m=1}^{N, M} \int_{F^{-1}\left(\frac{n-1}{N}\right)}^{F^{-1}\left(\frac{n}{N}\right)} \int_{F^{-1}\left(\frac{m-1}{M}\right)}^{F^{-1}\left(\frac{m}{M}\right)} e^{j2\pi\tau \left[f_{T_{max}} \cos(\beta_T^m - \gamma_T) + f_{R_{max}} \cos(\beta_R^n - \gamma_R) \right]} \right. \\ & \left. \times \frac{e^{k_T \cos(\beta_T^m - \mu_T) + k_R \cos(\beta_R^n - \mu_R)}}{4\pi^2 I_0(k_T) I_0(k_R)} d\beta_T^m d\beta_R^n \right. \end{aligned}$$

$$\begin{aligned} & \left\{ \frac{1}{4\pi^2 I_0(k_T) I_0(k_R)} \int_{-\pi}^{\pi} \int_{-\pi}^{\pi} \cos\left\{2\pi\tau \left[f_{T_{max}} \cos(\beta_T - \gamma_T) + f_{R_{max}} \cos(\beta_R - \gamma_R) \right] \right\} \right. \\ & \left. \times e^{k_T \cos(\beta_T - \mu_T) + k_R \cos(\beta_R - \mu_R)} d\beta_T d\beta_R, \quad (Case I) \right. \\ & \left. \frac{1}{2\pi^2 I_0(k_T) I_0(k_R)} \int_0^{\pi} \int_0^{\pi} e^{j2\pi\tau \left[f_{T_{max}} \cos(\beta_T - \gamma_T) + f_{R_{max}} \cos(\beta_R - \gamma_R) \right]} \right. \\ & \left. \times e^{k_T \cos(\beta_T^m - \mu_T) + k_R \cos(\beta_R^n - \mu_R)} d\beta_T d\beta_R, \quad (Case II) \right. \\ & \left. \frac{1}{4\pi^2 I_0(k_T) I_0(k_R)} \int_{-\pi}^{\pi} \int_{-\pi}^{\pi} e^{j2\pi\tau \left[f_{T_{max}} \cos(\beta_T - \gamma_T) + f_{R_{max}} \cos(\beta_R - \gamma_R) \right]} \right. \\ & \left. \times e^{k_T \cos(\beta_T^m - \mu_T) + k_R \cos(\beta_R^n - \mu_R)} d\beta_T d\beta_R, \quad (Case III) \right. \\ & \left. (15) \right. \end{aligned}$$

where at the third equality of (15), the integration variables θ_T and θ_R were replaced by $\beta_T^{m_i/q} = F^{-1}\left(\frac{m_i/q-1/2+\theta_T}{M_i/q}\right)$, $d\theta_T = \frac{M_i/q e^{k_T \cos(\beta_T^{m_i/q} - \mu_T)}}{2\pi I_0(k_T)} d\beta_T^{m_i/q}$, $\beta_R^{n_i/q} = F^{-1}\left(\frac{n_i/q-1/2+\theta_R}{N_i/q}\right)$, $d\theta_R = \frac{N_i/q e^{k_R \cos(\beta_R^{n_i/q} - \mu_R)}}{2\pi I_0(k_R)} d\beta_R^{n_i/q}$, $\beta_T^m = F^{-1}\left(\frac{m-1/2+\theta_T}{M}\right)$, $d\theta_T = \frac{M e^{k_T \cos(\beta_T^m - \mu_T)}}{2\pi I_0(k_T)} d\beta_T^m$, $\beta_R^n = F^{-1}\left(\frac{n-1/2+\theta_R}{N}\right)$, and $d\theta_R = \frac{N e^{k_R \cos(\beta_R^n - \mu_R)}}{2\pi I_0(k_R)} d\beta_R^n$. The definite integrals at the last equality of (15) can be solved by using the equality $\int_{-\pi}^{\pi} e^{a \sin c + b \cos c} dc = 2\pi I_0(\sqrt{a^2 + b^2})$ [13]. After some manipulations, the closed-form expression of the CF $\hat{\rho}_{\hat{h}\hat{h}}(\tau)$ can be obtained and is the same as $\rho_{hh}(\tau)$ in (2).